Catalysis Today 356 (2020) 349–358

Contents lists available at ScienceDirect

Catalysis Today

journal homepage: www.elsevier.com/locate/cattod

Obtaining of value added chemicals from catalityc dehydration of glycerol

Eduardo Santiago Vázquez[a], Julia Aguilar Pliego[a,*], Joaquín Pérez Pariente[b], Manuel Sánchez Sánchez[b], Ángel R. Arteaga Licona[a], Misael García Ruiz[c], Dora Solis-Casados[d]

[a] Área de Química Aplicada, Departamento de Ciencias Básicas, UAM-A, San pablo 180, C.P. 02200, Cd de México, Mexico
[b] Instituto de Catálisis y Petroleoquímica, CSIC, C/Marie Curie 2, Campus Cantoblanco, 28049, Madrid, Spain
[c] Facultad de Química, Universidad Autónoma del Estado de México, Paseo Colón Esquina Paseo Tollocan S/N, Toluca Estado de México, C.P. 50000, Mexico
[d] Personal académico adscrito al Centro Conjunto de Investigación en Química Sustentable, UAEM-UNAM, Mexico

ARTICLE INFO

Keywords:
Glycerol
Alumina
Ceria
Biofuels
Mixed
Oxides

ABSTRACT

Five catalysts were synthesized by changing the molar proportions (15, 30, 50, 70, 85 %) of ceria/alumina by the sol-gel method with nonionic surfactant (Tergitol 15-S-9), after they were impregnated with 1% weight Pt for evaluation in the dehydration of glycerol, modifying the W/F ratio (9.09, 13.63 and 18.18 gcat*h/mol). Through X-ray powder diffraction and also by X-ray photoelectron spectroscopy, the presence of ceria in the structure of alumina was identified. As the amount of cerium oxide increase, the BET surface area and the strength of the acid sites (TPD-NH_3) increased as well, in turn, the pore size (mesoporous) remained constant. The catalytic tests were carried out in the gas phase in a continuous-flow fixed-bed reactor, within which the ceria showed a positive effect on the performance of the samples, improving the levels of conversion and selectivity towards acetol, probably due to the contribution of acid and redox sites of ceria. On the other hand, as the molar ratio of ceria decreased, the selectivity toward acrolein increased, possibly resulting in the presence of Brnsted sites.

1. Introduction

Due to the existing environmental problematic about the exploitation, depletion and dependence of oil, for this reason, it is necessary to the development of energies able to satisfy the fuel demand, which is increasing day by day according to population growth [1]; one of alternatives that it has generated greater interest worldwide are renewables energies. Among which are the fuels from biomass (bio-fuels), as the biodiesel, during the process of its production, it may be obtained glycerin (10 % w) represents its main advantage. In the last decade, the biodiesel industry has had a significant increase due to rise in oil prices and the concern for energy security; this problematic has contributed to the large to excess glycerin in the world market [2–4].

According to recent statistics, the production of biodiesel in the United States of America has been increasing in the last decade, from 20 million gallons in 2003 to 1.8 billion gallons in 2013. For the year 2000, the total world production of biodiesel was of 0.8 billion gallons increased to 4 and 16 billion gallons in 2005 and 2010 respectively [5,6], according to OECD-FAO (Organization for Economic Co-operation and Development and the Food and Agriculture Organization) for the 2024 the global production of biodiesel will reach 39 billion gallons [7].

However, the glycerin from the transesterification of biodiesel is known as “crude glycerol”, which contains impurities such as methanol, methyl esters of fatty acids and salts residues of the transesterification reaction. Due to these impurities, the purification cost of crude glycerol is very high; consequently, the use in these traditional industries is not feasible despite its low market price [8–11].

The main uses of glycerol is in cosmetics, medicines and food products [5,12], in a lower percentage is in the production of antifreeze, despite having been replaced by ethylene glycol since the 1930s due to economic issues, due to the excess of glycerol in the global market caused by the increase in the production of biofuels, I present a possibility of obtaining an extra profit [12]. Most of the antifreeze is discarded in the sewage system, which generates an environmental problem [13].

It is estimated that the production of biodiesel will continue to raise, a situation that is not reflected in the demand for it; which produced a decrease in the price of glycerol. With these market conditions, it is necessary to find alternative ways to use glycerol as a raw material and be able to take advantage of it to obtain value-added products [14–16].

Some of the chemical reactions that may be performed to obtain value-added products are: selective oxidation, hydrogenolysis, dehydration, acetylation, carboxylation, decomposition, dehydroxylation, selective oligomerization, esterification and etherification; to mention a

* Corresponding author.
E-mail address: apj@azc.uam.mx (J.A. Pliego).

https://doi.org/10.1016/j.cattod.2020.06.056
Received 1 February 2019; Received in revised form 6 April 2020; Accepted 22 June 2020
Available online 29 June 2020
0920-5861/

few [17,18].

A promising option for the valorization of glycerol is through the dehydration reaction. This reaction is carried out, mainly, by acid catalysts, where it is possible to obtain mainly acrolein and acetol, which are important chemical products for the chemical and agrochemical industries, mainly in the textile industry, of paints. Glycerol can lead to the formation of acrolein on a variety of acid catalysts, such as sulfates, phosphates, metal oxides, heteropoly acids, and zeolites [19–21].

In previous researches have used different types of catalysts include: heteropoly acids and other supported inorganic acids [22–25], zeolites [26–28], sulphated zirconia [29] and mixed oxides [30–34], within which, according to the literature [35] oxide catalysts combine improvements in properties and greater catalytic activity than oxides in the same way studies carried out on alumina [36] and mesoporous ceramics [37], in which conversions higher than 80 % were obtained towards acrolein and acetol respectively.

Previous works on the dehydration of glycerol using mixed oxide catalysts report the synthesis of Al_2O_3, SiO_2, and TiO_2 supported catalysts Nb and W-oxide catalysts [38] obtaining an 80 % conversion, SiO_2/Al_2O_3 catalysts with maximum conversions of 54 % [39] and conversions around 70 % for the mixed oxides catalysts of Ce/Zr [40].

Alumina has the characteristics of textural properties as a high surface area that is necessary to have a high concentration of acid centers, as well as many suitable pores, large pore volume, thermal stability and amphoteric properties [41]. On the other hand, the ceria has redox and basic properties, thermal stability, dispersion improvement and support stabilization [42]. Cerium oxide-based mesoporous materials with pore sizes between 2 and 50 nm prepared through a template mechanism have received much attention in catalytic applications [3]. The CeO_2 has a crystalline structure like fluorite (CaF_2). The presence of highly reducible Ce^{4+} and Ce^{3+} species, a high proportion of oxygen surface defects and acid-base properties make CeO_2 suitable for catalytic applications [43]. V. González and co-workers [44], reported the synthesis of nanoporous aluminas in the presence of nonionic surfactants, using chelating ligands to chemically modify the aluminum alkoxide precursor and using 1,4-dioxane as solvent and/or a different nonionic surfactant (Tergitol 15-S-9 and Tergitol 15-S-15). Based on the above, in the present work, catalysts of mixed oxides of alumina and ceria using the sol-gel method used by González, V., et al. with some variations like the solvent [44]. These mixed oxides are impregnated with Pt as a hydrogenating metal to prevent deactivation of the catalysts, as well as an improve the activity and selectivity of the reaction products.

In order to determine the catalytic activity of these mixed oxides with its structural characteristics and with the active sites presents in these materials, they were evaluated in the dehydration reaction of glycerol to obtain products of value added as acrolein and acetol.

2. Experimental

2.1. Materials

The reagents used for mixed oxide synthesis were aluminum sec-butoxide (97 % purity, Acros), nitrate of cerium hexahydrate (99 % purity, Sigma-Aldrich). Tergitol 15-S-9 (Sigma -Aldrich) was used as a surfactant and like solvent was sec-butanol (99 % purity, Sigma-Aldrich). $Pt(NH_3)_4(NO_3)_2$ (99 % purity, Sigma-Aldrich) precursor salt. Acetol, acrolein, acetaldehyde, propanal, allyl alcohol and 1–2 propanediol standards organic compounds (Sigma Aldrich) in the activity test.

2.2. Synthesis of catalysts

Based on the sol-gel method for the synthesis of mesoporous alumina [44], which was modified to synthesize the 5-mixed oxide alumina/ceria catalysts, being the molar ratios, according to Eq. 1:

Table 1
Theoretical and experimental molar ratios of all samples (EDS).

	Theoretical [fraction mol]		EDS [fraction mol]	
Catalytics	Ceria	Alumina	Ceria	Alumina
AC-15	0.15	0.85	0.17	0.82
AC-30	0.30	0.70	0.27	0.73
AC-50	0.50	0.50	0.49	0.51
AC-70	0.70	0.30	0.75	0.25
AC-85	0.85	0.15	0.88	0.12

$$\mathbf{1.0}[x\ (Ce(NO_3)_3{*}6H_2O) + y(C_{12}H_{27}O_3Al)]{:}\mathbf{0.1}S{:}\mathbf{2.0}H_2O{:}\mathbf{18.2}\ C_4H_{10}O] \quad (1)$$

Where:

x = Molar fractions of ceria, using as precursor aluminum sec-butoxide

y = Molar fractions of alumina, using as precursor nitrate of cerium hexahydrate

S = Surfactant: Tergitol 15-S-9

$C_4H_{10}O$ = Solvent: Butanol

The molar fractions of each oxide are in Table 1; the method consists of preparing a solution 1, dissolving Tergitol 15-S-9 in sec-butanol then aluminum sec-butoxide was added (according to the molar ratio) undergoing constant agitation for 30 min. On the other hand, solution 2 was carried out by mixing distilled water with sec-butanol, later the solution 2 was added dropwise (1 mL/min) to solution 1, observing the formation of the gel. Subsequently cerium nitrate hexahydrate is added in the corresponding molar ratio. The gel was allowed to age 24 h at 55 °C then washed with ethanol and for the removal of the surfactant Soxhlet extraction was used with ethanol at 100 °C for 24 h, then dried at room temperature and calcined with flow of air at 550 °C for 4 h at 2 °C/ min.

The impregnation of Pt was carried out by the incipient wet impregnation technique [45] the precursor salt of $Pt(NH_3)_4$ $(NO_3)_2$ was used. The calculations were made to disperse 1 wt% of platinum in 1 g of support. The salt was dissolved in the catalyst, it was calcined with a ramp of 5 °C/min at 400 °C for 4 h and for the reduction a ramp of 5 °C/min was used up to a temperature of 300 °C with air flow and the temperature was maintained for 1 h with H_2 flow. The nomenclature used was AC- (molar fraction of ceria); all samples were impregnated with Pt. Unsupported catalysts without platinum AC-85 and AC-15 were denoted as AC-85 S and AC-15 S, respectively.

2.3. Characterization

Several characterization techniques were used to determine the properties of the catalysts: the surface area was calculated with the BET method; the pore size distribution and average pore size were estimated by the BJH analysis method applied to the desorption branch of the isotherm (ASAP 2020 Micromeritics Telurio). The crystal structure of the samples was evaluated by X-ray diffraction (XRD) (Polycrystalline X-ray diffractometer X'Pert Pro PANalytical). The crystal size was estimated using the Scherrer equation of the most intense X-ray diffraction signal. The acidity of the samples was measured through a programmed temperature desorption of NH_3 (TPD) (Model BELCAT-B (BEL Japan Inc.)). The calcination temperature and the control of the amount of surfactant were measured by means of the Termogravimetry (TGA) (Perkin Elmer (TGA 7) and infrared spectroscopy (IR) (Nicolet 5ZDX FTIR spectrometer, equipped with an MCT detector (Mercury, Cadmium and Tellurium)) was used to measure the presence of organic compounds. To consider catalyst morphology, it was observed by scanning electron microscopy (SEM) (Desktop Scanning Electron Microscope Hitachi and model TM-1000). X-ray photoelectron

spectroscopy (XPS) was done to analyze changes in the chemical environment of atoms, analysis was done in a JEOL JPS 9200 equipment using an Al Kα source, high resolution spectra were acquired for each element, taking C1 s signal in 284 eV to adjust the charge displacement. Elemental chemical composition of catalysts was determined using the corresponding sensitivity factors.

2.4. Catalytic testing

The catalysts were evaluated in the dehydration reaction of glycerol in gas phase in a fixed-bed continuous flow reactor, which operated at atmospheric pressure. The reaction system was made up of an evaporator, a reactor and a condenser. The feed concentration was 10 % in glycerol at a rate of 10 mL/h with a flow of N_2 (30 mL/min.) as a carrier gas; the mixture enters the evaporator, which is at 300 °C temperature, obtaining a change of phase. The steam phase is passed through to the fixed bed reactor at 355 °C; the products are taken in the condenser in liquid form for their later analysis. The W/F ratio, was changed with 3 values (9.09, 13.63 and 18.18 gcat*h/mol). The quantified and analyzed reaction products were: acetol, acrolein, acetaldehyde, propanal, allyl alcohol and 1–2-propanediol. Calibration curves were made with the respective standard product. The products analyzes were made in a Perkin Elmer chromatograph, which has a flame ionization detector using a chromatographic column "HP Innowax" (30 m x0.25 mm x0.25 μm).

3. Results and discussions

3.1. X-ray powder diffraction

Fig. 1 shows the diffraction patterns of the samples synthesized where the successful synthesis of the mixed oxides is confirmed. The characteristic peaks of the cerium oxide DRX in the planes: (111), (200), (220), (311), (222), (400), (331), (420) and (422); where each one corresponds to the following angles 2θ: 28.6, 33.2, 47.4, 56.4, 59.1, 69.4, 76.8, 79.1 and 89.9, while for the case of alumina the characteristic peaks in angle range 2θ of 30–50 they are transposed with those of the ceria, being the peak of 440 in the angle 2θ of 67.1, this is the only peak of the alumina that can be observed in the samples, added to the amorphous form that alumina [46]. Because the ceria presents a fluorite (crystalline) type structure. The reflections that belong to the cerium oxide become more intense. The absence of a Pt diffraction peak may be explained, since the metal is very dispersed in the catalyst and this is in small quantities, that are outside the detection limit of the technique, indicating that the Pt does not in large crystalline aggregates [47]. The correspondence of the interplanar angles of the diffractograms of the mixed oxide samples with that of the cerium oxide, supposes the absence of the alumina inside the crystalline fluorite structure of the ceria [48] giving an indication of a structural arrangement on the framework of the crystalline structure.

3.2. Scanning electron microscopy

Using the SEM technique (Fig. 2), the presence of amorphous solids may be observed, this may be due to the crystallinity of the oxides involved, since aluminum oxide generates layers that have an orthorhombic laminar structure where the oxygen atoms have a compact cubic packing [41,42]; while cerium oxide has a fluorite crystalline structure, where the Ce cations are located in a cubic structure centered on the faces with the anions or placed inside the unit cell in a simple cubic arrangement. In Table 1 shows the results of the practical compositions determined by energy dispersion spectroscopy (EDS), in which there are not significant differences with respect to the theoretical ones.

3.3. N_2 adsorption

The increase in the specific surface area of the catalysts combined with moderate acidity was correlated to the conversion of glycerol and the selectivity of acrolein. The Fig. 3 shows the adsorption-desorption isotherms of the catalysts, resulting in a type IV isotherm, this one is typical of mesoporous materials. This isotherm is typical of wide mesoporous solids associated to irreversible phenomena of condensation and capillary evaporation inside the pores and a cycle of hysteresis type H2 for pores in the shape of an inkwell (with a wide cavity and surrounding narrowness or necks) with porous materials quite regularly with a fairly narrow pore size distribution [48].

With respect to the surface area and the pore volume of the catalysts (Table 2), a direct relationship may be observed with the amount of ceria present in the structure; the greater the amount of ceria, the

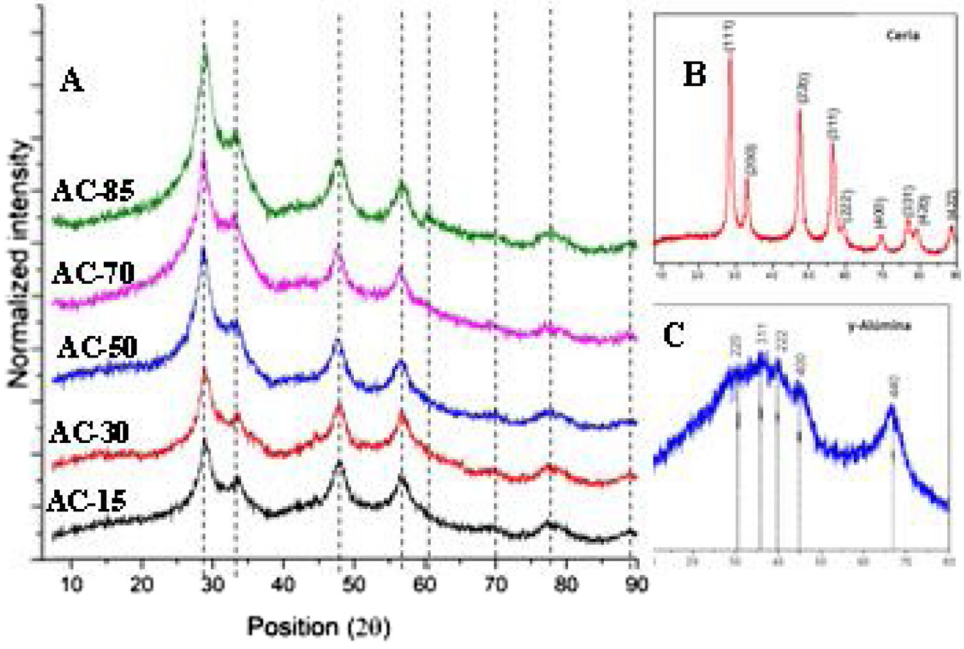

Fig. 1. DRX patterns of samples (A) and DRX patron patterns of ceria(B) and alumina(C).

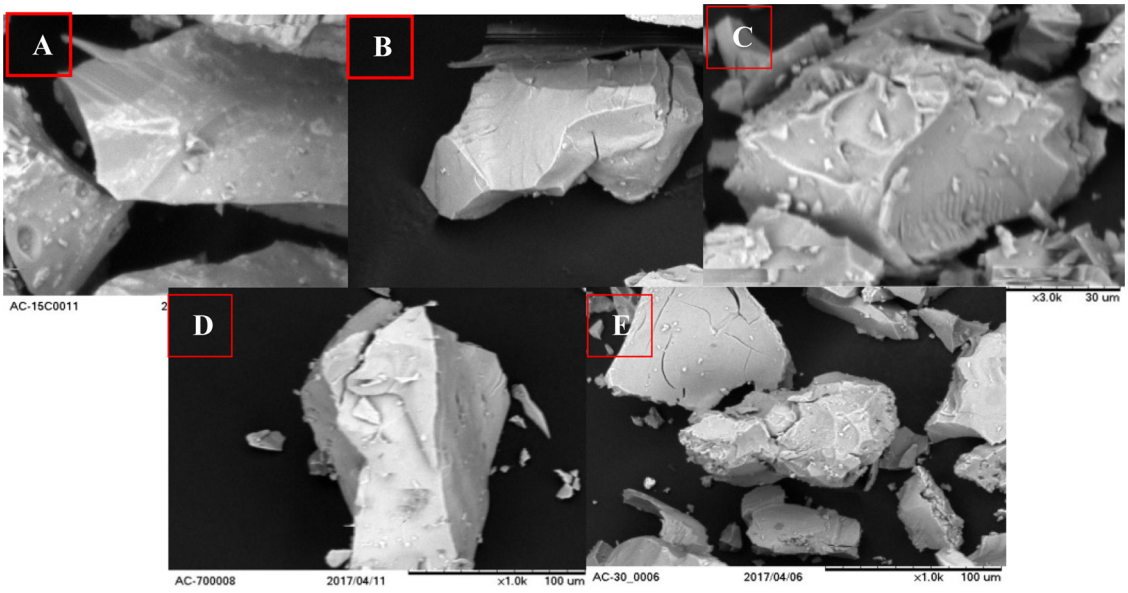

Fig. 2. SEM micrographs: AC-15(A), AC-30(B), AC-50(C), AC-70(D) and AC-85(E).

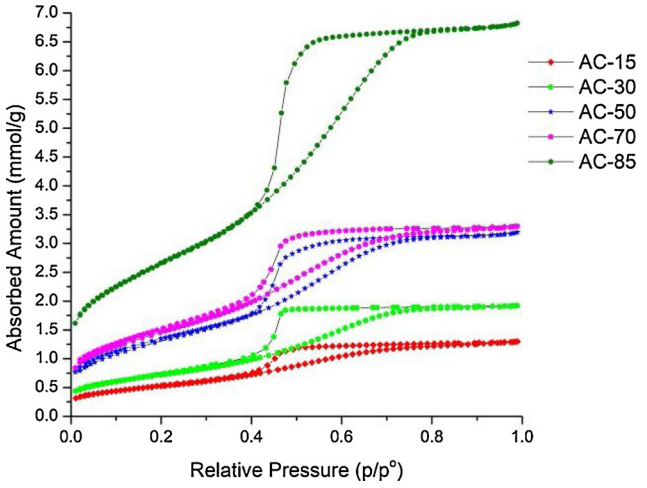

Fig. 3. Nitrogen adsorption results obtained for each sample.

Table 2
Textural properties.

Catalysts	Surface Area (m^2/g)	Pore Size (Å)	Pore Volume
AC-15	42.5	4.37	0.0458
AC-30	58.2	4.56	0.0677
AC-50	108.2	4.07	0.1124
AC-70	118.9	3.83	0.1181
AC-85	212.8	4.43	0.2407

greater the surface area; being that, alumina is a simple oxide widely used as a catalyst for its high surface areas [44], so, the interaction between both oxides generates a structural arrangement that generates this tendency, which may be due to the formation of roughness on the catalyst surface. The isotherm of the sample AC-85 is the one that presents the highest adsorption of N_2, this has the largest surface area. All the mesoporous metal oxides displayed BET surface areas, pore volumes and sizes larger than that of the bulk oxides [49].

On the other hand, the pore size remained constant around 4 nm, with the effect of the surfactant to have uniformity of the pores, classifying them as mesoporous materials. The surface area and pore size distribution improves in these materials the diffusion of reactive compounds and reaction products and facilitates the dispersion of a transition metal such as platinum when used as a catalytic support [38]. In their study, glycerol conversion increased due to reduced surface acidity strength and increasing mesoporosity improving the accessibility of glycerol to active sites.

3.4. Temperature-programmed desorption (NH-TPD)

The TPD-NH_3 results of the samples are presented in Table 3. According to Tanabe and coworkers [50] the strength of the acidic sites of the solids within TPD profiles can be classified by the ammonia desorption temperature as weak (120–300 °C) and strong (500–650 °C). Ammonium adsorption capacity is a measure of surface acidity especially weak acidity, decreased with increasing ceria percentage in mesoporous ceria–alumina samples, on the other hand, there is an increase in the total acidity of the catalyst as the amount of ceria increases, this may be due to the fact that the ceria performs a higher contribution of Lewis-type acid sites, while gamma-alumina contains Bronsted-type acidity [29]. The NH_3 uptake changes from 1.35 $mmolg^{-1}$ for AC-15 to 0.89 $mmolg^{-1}$ for AC-15, indicating less acid sites, the total acidity initially increased with the alumina content. Therefore, the AC-85 catalyst contains a greater amount of Lewis acid sites probably and expected to have the highest conversion of glycerol to acetol. According to some findings, Al_2O_3 possesses both Bronsted and Lewis acid sites of weak to strong strength, however, the diminution of the strength of the Lewis acid sites (AC-15) could be due to the replacement of the Al^{3+} ions by the more electronegative Ce^{4+} ions, as was the case for the mixed oxides [51,52].

Table 3
Acidic strength of the catalysts(TPD).

Catalysts	mmol NH_3/g		
	Weak Acidity (100 − 300 °C)	**Strong Acidity (500 − 700 °C)**	**Total**
AC-15	0.0672	0.8324	**0.8995**
AC-30	0.0236	1.1952	**1.2188**
AC-50	0.3731	0.8479	**1.2210**
AC-70	0.3073	1.0386	**1.3460**
AC-85	0.3190	1.0341	**1.3532**

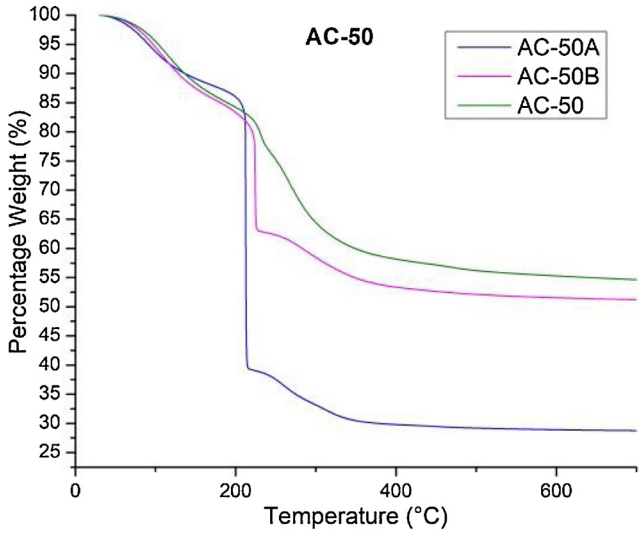

Fig. 4. TGA of AC-50A (before the extraction), AC-50B (after the extraction) and AC-50 (48 h of the extraction).

3.5. Infrared spectroscopy

The IR spectra of the samples presents the characteristic bands of gamma-alumina and Ce-O (spectra not shown). We observe a band around the 650 cm^{-1} that corresponds to the stretch of the Ce-O bond [53], as well as, a small peak is shown at 400 cm^{-1} that may correspond to the presence of gamma-alumina [54]; when comparing the five catalysts no significant difference is shown, so that the structure of these remains constant. The absence of peaks in the range of 4000 to 1000 cm^{-1} is due to the adequate elimination of contaminants such as: surfactant, wash ethanol residue, butanol (solvent).

3.6. TGA and DTA analysis

The temperature of calcination and the elimination of the TG (Tergitol) of the extracted samples were studied by TGA. In the Fig. 4, the sample AC-50A (before the Soxhlet extraction) shows a sudden fall around 200 °C causing the loss of almost 70 % of the sample, this is due to the decomposition of the surfactant causing break the structure of the catalyst, the sample AC-50B was obtained after 24 h of extraction, showing the same behavior but on a smaller scale, so a second extraction cycle (AC-50) was carried out, eliminating the sudden fall of thermogram from the sample. Based on this, the samples AC-70 and AC-85 were made with an extraction time of 48 h.

The thermograms (Fig. 5) shows a first weight loss step, up to approximately 100 °C, that corresponds mainly to the desorption of water, followed by two faster steps with maximum slope at 200 and 300 °C, respectively, they are related to the remains of organic compounds; the first loss is related to the surfactant (Fig. 5) and the second to the solvent and remains of the aluminum precursor salt, so that its decrease can be presumed to be related to the amount of alumina present in the sample.

This technique can provide information on the structure of simple metal oxides, which is obtained by calculating the theoretical weight of the catalyst; however, for the case of mixed oxides, they have various interactions between the oxides present, making it impossible to obtain of this data by this technique.

3.7. X-ray photoelectron spectroscopy (XPS)

The ceria-alumina interaction in prepared catalysts was analyzed taking the wide spectra to get a complete idea of the elements in the surface of samples. The narrow spectra of Ce, Al, O 1s and C 1s were taken to determine chemical shifts in a photoelectron spectrum. The taken spectra were used for estimating the chemical state of the elements and determine the shifts in binding energy correlating them with its chemical environment, elucidating the interaction amongst Ce and Al. Fig. 6 I) shows the spectra of the cerium 3d5/2 region for all catalysts, including a reference sample of CeO_{2-x}, from this figure can be observed a broad doublet with peak centered around of 884 and 903 eV. The Ce 3d5/2 region was deconvoluted for each catalyst, at least three doublets were obtained in this region, for each catalyst (Table 4).

It is observed in Fig. 6 I) spectrum a) that Ce has the oxidation state 2+, it is assumed for the doublet located at 881.2 and 900.9 eV. This doublet is in a major proportion in catalyst AC-30. This doublet has a slight shift at 882.9 eV in catalyst AC-50 (Fig. 6 I spectrum b). The peak appears in 880.9 eV in catalyst AC-85 (Fig. 6 I spectrum c). Proportions of this peaks are in Table 4.

The second doublet located around of 884 and 903 eV was attributed to the Ce in its 3+ oxidation state. The sample AC-30 shows the main peak at 884.6 eV (Fig. 6 I spectrum a), the AC-50 catalysts at 886.3 eV (Fig. 6 I spectrum b) and AC-85 catalyst shows this peak at 884.78 eV (Fig. 6 I spectrum c). The third doublet is peaking at 889 and 909 eV, attributed to the Ce in its 4+ oxidation state. The sample AC-30 shows the main peak at 887.9 eV (Fig. 6 I) spectrum a), the AC-50 catalysts at 889 eV (Fig. 6 I spectrum b) and AC-85 catalyst shows this peak at 888.0 eV (Fig. 6 I spectrum c). The unsupported CeO_2-x sample has an intense peak for the Ce3d5/2 around of 884.6 eV attributed to Ce_2O_3 the other peak of this doubles is located at 903 eV. It is important to note that with the increase in Ce content in catalytic formulation a small peak become to appear located in 894.6 eV in catalyst AC-50 and located at 893.7 eV in the AC-85 catalyst (Fig. 6 I spectra a and b), this peak can be attributed to the interaction between Ce-Al, this peak is absent on the unsupported CeO_2-x spectrum. Analyzing Al 2p3/2 region

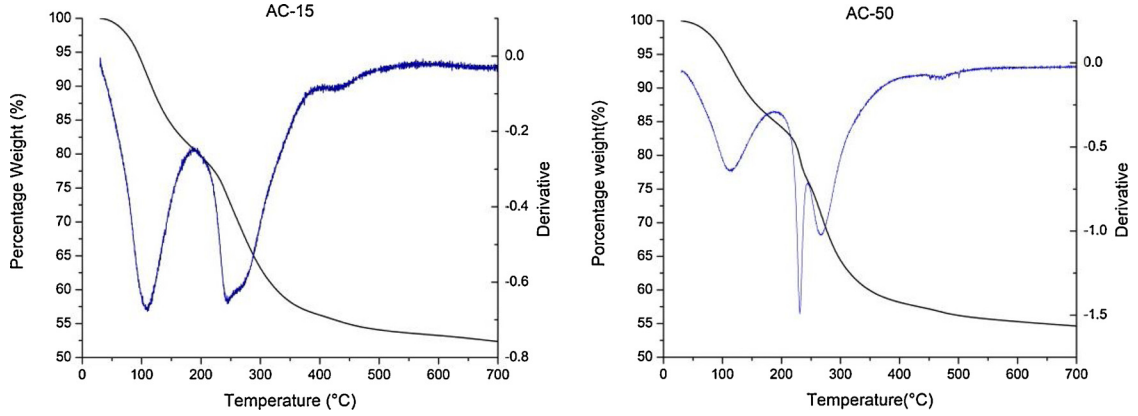

Fig. 5. TGA of samples: AC-15, and AC-85 (before the extraction).

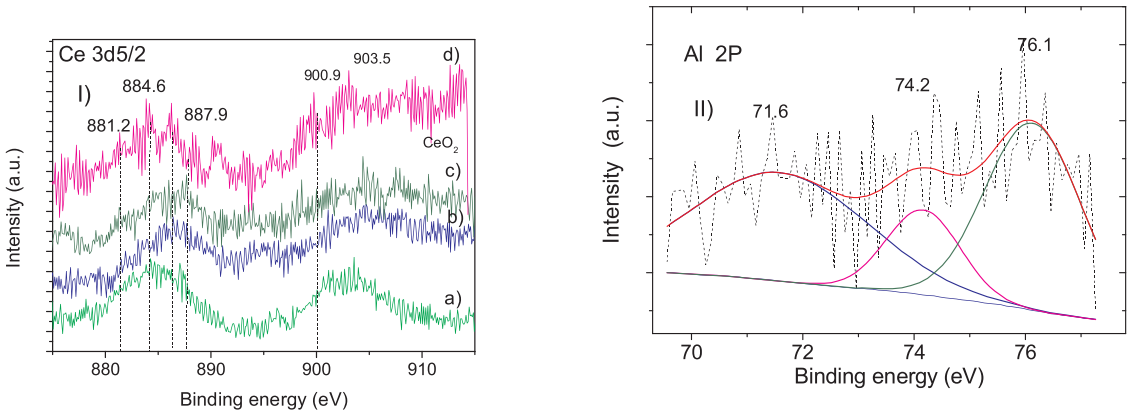

Fig. 6. I) XPS spectra, Ce 3d5/2 region for a) AC-30, b) AC-50, c) AC-85 and d) CeO_2-x catalysts. II) XPS spectrum of Al 2p3/2 region.

in catalysts (Fig. 6 II), it was also corroborated the interaction of Al and Ce, due to the small peak observed at 76.1 eV, interactions amongst Ce and Al are expected since the preparation technique used is the sol gel technique, which is useful to get mixed oxides.

On the other hand, chemical states of the Pt species in the catalysts were analyzed by XPS and results of the distribution of oxidation states of the platinum species of of the AC-30, AC-50 and AC-85 catalysts are shown in Table 5. Literature values reported for the Pt $4f_{5/2}$ level of platinum different oxidation states are as follows [55]: Pt°, 315.5 eV, PtO, 318.4 eV; PtO_2, 320.9 eV and $PtCl_4$, 323.6 eV. The Pt 4f 5/2 peak at 315.5 eV confirms that majority of Pt exists in elemental state in all samples. In addition, it is observed that if the amount of Ce increases, the amount of elemental Pt° increases [62].

Table 5
Proportions of Pt specie, obtained from deconvoluted spectra of XPS of Pt 4f 5/2 region.

Catalyst	Signal (eV)			
	315.5	318.4	320.9	323.6
	Pt^0	**PtO**	**PtO_2**	**$PtCl_4$**
	% Pt specie			
AC-30	15	24.9	38.6	21.5
AC-50	20.9	44.2	6.81	28.12
AC-85	40.51	8.0	26.7	24.9

3.8. Catalytic activity

The ceria-alumina catalysts (Pt 1 wt%) were catalytically evaluated in the dehydration reaction of glycerol in gas phase at 355 °C. A 10 % wt. glycerol-water solution was fed to the reaction system with a feed flow of 10 mL/h with different W/F values (9.09, 13.63 and 18.18 gcat*h/mol). Five catalysts of mesoporous mixed alumina/ceria oxides were synthesized at different molar ratios by means of the sol-gel method for the synthesis of mesoporous alumina [44]; which was adequate for said catalysts, which showed an increase in surface area according to the amount of ceria, in the same way, the number of acidic sites increased, so that the AC-85 catalyst presented the best characteristics catalytically speaking.

The results of the catalytic tests for the conversion of glycerol showed the addition of ceria in the alumina structure had a positive effect in terms of activity. The AC-85 catalyst presented significantly higher conversion values, which could be associated with the presence of a greater surface area and acidic sites and presumably basic sites that could be caused by the contribution of each oxide in the structure.

According to the dehydration reaction of glycerol, more than ten products can be obtained [15], of which were quantified: acrolein, acetol, allylic alcohol, acetaldehyde, propanal and 1,2 propanediol; being those that have been reported in previous works that show higher selectivities [36,37]. Fig. 7 shows the distribution of products for samples AC-85 and AC-15; A significant difference was observed in the selectivities of acetol and acrolein. Formation of the main reaction products, acrolein and acetol, is initiated by dehydration involving protonation of either secondary or primary OH groups respectively [22]. In the sample AC-15 (greater amount of alumina) is observed the obtaining of a greater quantity of acrolein (selectivities superior to 35 %) and in smaller amount the acetol. For the case of the sample AC-85 presents an inverse tendency, greater selectivity towards acetol (around 40 %) than to acrolein (greater than 15 %), with respect to the other quantified products, they did not present a significant difference in the distribution in the catalysts synthesized, so that obtaining them does not depend directly on the presence of Bronsted or Lewis acid sites [56]. A. Kinage and cowokers [57] studied Na/Ceria and Na/alumina and other catalysts systems. The proposed mechanism for formation of acetol over acidic and basic sites. On acidic site first dehydration of glycerol occur followed by selective acetol formation. However, over basic site first dehydrogenation of glycerol occurs followed by dehydration of glycerol leading acetol. Equally, H.S.A. De Sousa and

Table 4
Proportions of cerium oxide with different oxidation state, obtained from deconvoluted spectra of XPS of Ce 3d5/2 region.

Catalysts								
		AC-30			AC-50		AC-85	
Ce specie	Oxidation state	Peak position (eV) 3d5/2						
				%specie		%specie		%specie
CeO	Ce^{2+}	881.1	900.9	23.9	882.9	21.8	880.8	19.1
Ce_2O_3	Ce^{3+}	884.6	903.5	56.7	886.3	52.4	884.7	47.1
CeO_2	Ce^{4+}	887.9	909.8	19.3	889.3	20.9	888.0	29.0
					894.6	4.8	893.2	4.62

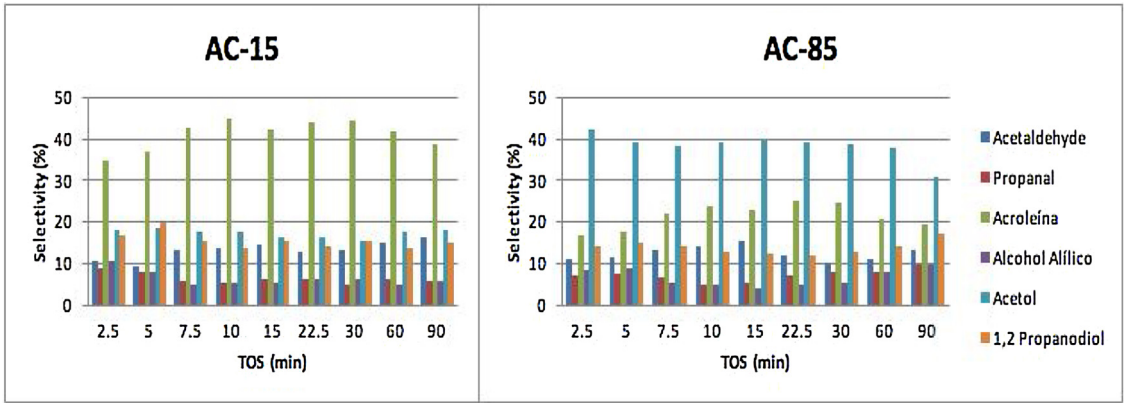

Fig. 7. Distribution of selectivity vs time of AC catalysts W/F = 18.18 gcat h/mol to 355 °C reaction temperature.

coworkers [51] studied ternary mixtures of metal-oxide catalysts in the glycerol dehydration reaction. They prepared mixed oxides based on ceria (CeO_2), and catalyst was found quite selective in the dehydration of glycerol, but rather towards acetol (60 %) instead of acrolein (40 %). In a similar work S.J. Vasconcelos and coworkers [43] obtained mixed oxides CeO_2 with high surface area and mesoporous structure. It is noteworthy that the conversion was strongly depending on the catalyst and acid-base properties. The authors admit that the preparation method had a significant influence on the particle size and the homogeneous distribution. In our case, as the amount of ceria increases with respect to alumina, acetol production increases, mainly due to the presence of basic and Lewis acidic centers [58], which is in agree with what was reported by the mentioned above authors. If we take as a basis the statement by De Sousa that says: a) glycerol is converted into acrolein due to Bronsted acid sites (alumina), b) acetol can be produced with basic sites or Lewis acid sites (ceria) and c) and the various secondary products are produced by parallel or consecutive reactions involving glycerol (Ce/Al).

Table 6 shows the selectivities of the samples AC-15 and AC-85 with platinum and without platinum at ≈30 % of conversion. Note that the contribution of platinum to short reaction times practically does not contribute. However, at higher times, the increase in conversion is significant Fig. 10. According to the study by E. Bozga and coworkers [59] high selectivities of 1,2-propanediol can be obtained from glycerol using platinum catalysts supported on metal oxides such as SiO_2 and alumina. Similarly, V. Montes and coworkers [58] mentioned that some catalysts impregnated with a low amount of transition metals, such as Pt and Pd, can obtain high selectivities of 1,2-propanediol, through the dehydration reaction of glycerol.

Given the high selectivities presented towards acrolein and acetol, in Fig. 8a and b their selectivities are shown for each of the catalysts synthesized at the W/F feed ratio differences of acetol and acrolein, respectively, where the relation between the amount of ceria and alumina present in the catalyst with acetol and acrolein respectively; in turn, related to the active sites, being the Bronsted type acid sites associated with the production of acrolein and the Lewis-type acid sites and redox sites to the formation of acetol [22]. With the characterization methods and the results, they revealed that with the synthesis of mixed oxides they lead to the formation of larger mesoporous pores, decreasing the support basicity, and limiting the production of undesired side-product such as coke. On the other hand, the effect of the W/F ratio is shown, where the highest values of selectivity and conversion are presented in W/F of 18.18 gcat*h/mol; which favors the conversion of the reaction, due to the presence of a greater number of acidic sites within the catalyst. The formation of allyl alcohol can be due to consecutive or parallel dehydration and reduction reactions, in which the enol intermediates in the presence of the redox catalyst resulted in a higher allyl alcohol selectivity [60]. The propanal, 1,2-propanodiol and acetaldehyde were products due to the hydrogenation of the C=C double bond by a consecutive gas-phase reaction. According to the literature [60], a pathway for glycerol conversion was proposed considering consecutive or parallel dehydration-reduction reactions with the participation of both acidic and redox sites.

Based on the above, in Fig. 9 the conversions of the five catalysts against W/F are shown, obtaining conversions higher than 80 % at a time between 10 and 20 min of catalysis, being the catalyst AC-85, the one that presented a conversion around 98 % in a time of 12.5 min. In the 90 min conversions may be observed that are between 40 and 60 %, showing a tendency towards deactivation of the catalyst. The deactivation phenomenon can be explained by the formation of coke. It shows that increasing the number of strong acid sites leads to rapid deactivation of catalysts due to the formation of carbonaceous deposits (Table 4), and the formed coke blocks the surface-active sites for further reactant adsorption, since these promote the decomposition of the molecule into low molecular weight compounds avoiding the interaction between glycerol and the acid sites of the catalyst. To avoid this phenomenon, Pt samples were impregnated, which prevents the formation of coke and lengthens the life of the catalyst. Therefore, the amount of impregnated Pt was not enough to prolong the life of the catalyst; the catalysts were evaluated before impregnation, obtaining maximum conversions of 50 % at short times. The unsupported catalysts AC-85 S and AC-15 S had low conversions with a W/F of 18.18 gcat*h/mol shown in Fig. 9. At 355 °C the catalyst AC-85 S showed a lower conversion of the 60 % and decrease to 25 % after 90 min of reaction. The catalysts with platinum have a better catalytic activity in terms of conversion and selectivity in comparison with catalysts without platinum. Since in these materials the conversion decreases by approximately 40 % in conversion. In the same case with the AC-15 S catalyst, presenting a maximum conversion at short times of 50 % and decrease to 15 % at 90 min. With the foregoing it can be said that the incorporation of platinum in these cerium/alumina oxide materials improves the catalytic activity in terms of conversion and selectivity

Table 6
Distribution of reaction products of AC-15 and AC-85 catalysts in the conversion of glycerol. Conditions: TOS 2.5 min, W/F 18.18 gcat*h/mol, 355 °C R.T, Conversion ≈.30 %

Products	Catalysts			
	AC-15	**AC-15 S**	**AC-85**	**AC-85 S**
Acetaldehyde	11.28	5.08	11.43	10.00
Propanal	8.58	10.17	6.64	11.67
Acrolein	34.92	38.98	16.82	31.67
Allilic alcohol	10.45	8.47	8.43	8.33
Acetol	17.93	20.34	42.13	25.00
1,2 propane diol	16.84	16.95	14.55	13.33

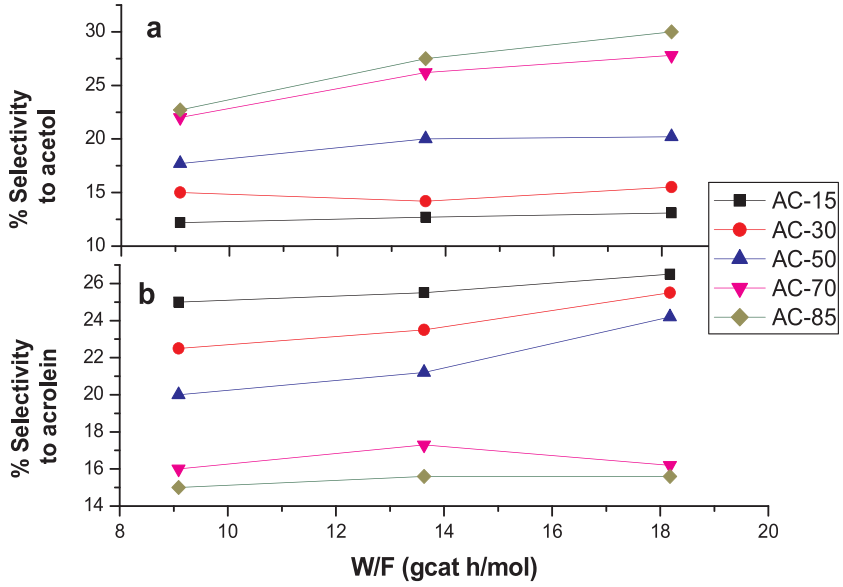

Fig. 8. Selectivity to acetol (a) and acrolein (b) vs W/F to 355 °C reaction temperature.

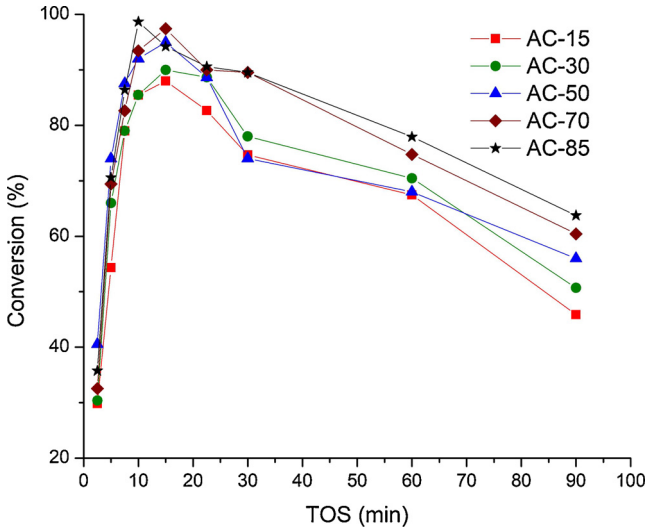

Fig. 9. Conversion of glycerol for each catalyst to W/F = 18.18 gcat h/mol and to 355 °C reaction temperature.

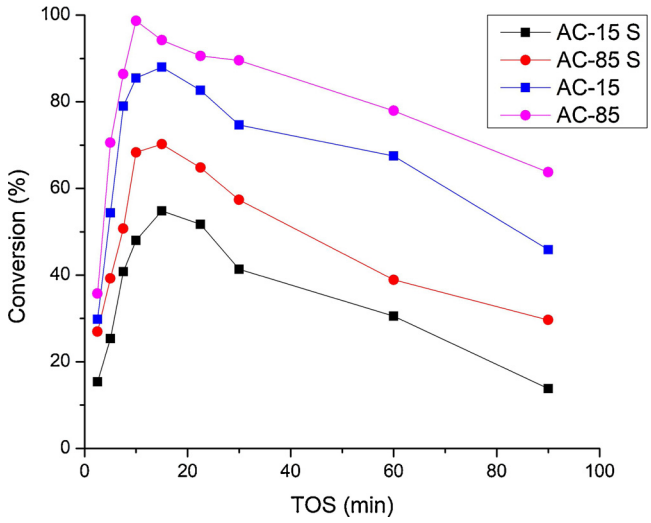

Fig. 10. Comparison of glycerol conversion over AC15 and AC85 catalysts with and without Pt (S) at W/F = 18.18 gcat.h/mol and to 355 °C reaction temperature.

(Table 6) [61,48]. As mentioned, catalysts of metal oxides such as alumina and ceria have been used in the dehydration reaction [36,37]. From which a comparative study was carried out on the selectivities for acrolein and acetol ().

The Fig. 11, with the results in this work with the ratio feeding W/F of 18.18 gcat*h/mol, we observe the selectivity points to acetol (red curve), it is shown that when you have pure ceria, the highest selectivity to this compound occurs. Which leads us to think about the presence of basic centers present in the ceria [63]. In the case of alumina (black curve) the highest selectivity to acrolein is when you have pure alumina. It is known that alumina has Lewis-type acid centers that could be the responsible of the formation of acetol [60]. Where it can be observed (Fig. 11) that there is a linear trend in the amount of acrolein and acetol obtained: "Greater amount of acrolein formed, more amount of alumina is in the sample", in the opposite way: "Greater amount of acetol, greater amount of ceria exists "; therefore, this relationship between mixed oxides and the main products of glycerol dehydration is explained by the presence of active Lewis and Brönsted acid centers in alumina, redox-basic in ceria, which predominate or which interact amongst them, probably when Ce/Al ratios change. There is the possibility of both OH groups in glycerol could be interacting with the surface of mixed oxide as observed by Sato and coworkers [64]. When the protonation is in the terminal hydroxyl group from glycerol, acrolein is obtained. Then, Ce^{+4} can be reduced by the eliminated hydrogen radical in the catalytic cycle and both OH groups in glycerol could be interacted with the surface of CeO_2–Al_2O_3 phase [51]. Moreover, this phenomenon represented a clear example of how the acid–base properties of solids could be adjusted by modifying the interaction of ceria and alumina phase obtained using this synthesis method. It is also important to emphasize that is possible that the incorporation of Al into the CeO_2 structure gets sites with stronger basic character, this is assumed from the electronegativity of the aluminum higher than the cerium possess, this was expected since the incorporation of aluminum into the CeO_2 atomic structure causes a change in the chemical environment as was found through XPS analysis, the shift in binding energy and also deconvolutions of Ce 3d5/2 and Al2P3/2 regions correlates well with the presence of stronger acidic and also basic sites and the catalytic performance observed. The catalytic activity of the Pt is not very pronounced since the deactivation of the catalysts is not

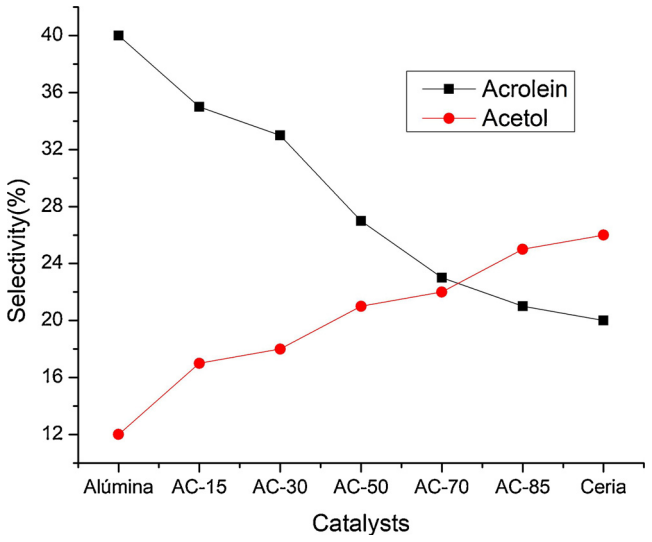

Fig. 11. Comparison between metal and mixed oxide catalysts (with Pt) to W/F = 18.18 gcat.h/mol and to 355 °C reaction temperature, at 10 min of TOS.

diminished by its presence. However, the Pt contributed in a small measure to improve the catalytic activity and very little in the selectivity of 1,2-propanediol.

4. Conclusion

The catalysts synthesized based on ceria and alumina were synthesized satisfactorily starting from the sol-gel method for mesoporous alumina, obtaining a new method for their synthesis, which showed a positive effect in improving the performance of the catalysts to obtain high conversion and selectivity values. Acid sites were identified on surfaces of mixed oxides by NH_3-TPD. These surface acid sites increased with increasing concentrations of alumina and decreased with increasing ceria concentration. The interaction between ceria and alumina promoted the generation of acidic Lewis, Bronsted, as well as basic and redox sites; as well as a structure presumably with folds on the surface, causing the increase in surface area as the amount of ceria increased; being the catalyst AC-85 the one that obtained better conversions and selectivity towards the acetol, in turn, the catalyst AC-15 presented greater amount of obtained acrolein, attributed to the presence of acidic sites of Bronsted type. The AC-85 catalyst showed a conversion of 98 % at a time of 10 min with a W/F of 18.18 gcat*h/mol. The selectivity to acetol increased with the ceria content, which can be again attributed to the Lewis acidity and/or basic sites of ceria.

The samples show strong acid sites, which favor the formation of coke in the sample, on the other hand, the lifetime of the catalyst was not as expected, if the Pt did not contribute to the elimination of coke. However, the Pt contributed in a small measure to improve the catalytic activity and very little in the selectivity of 1,2-propanediol.

By changing the amount of ceria and alumina in the series of catalysts studied, it is proposed that the active centers in the ceria are the stronger basic sites and acid Lewis sites to give acetol, and in alumina Brönsted centers to give acroleina (Fig. 11). The characterization of the series of catalysts must be deepened in order to better understand their structural properties, in order to know the way in which each of the oxides is in this mixture.

Declaration of Competing Interest

The authors declare that they have no known competing financial interests or personal relationships that could have appeared to influence the work reported in this paper

Acknowledgments

We thank CONACYT for the scholarship for the research stay of the student E. Santiago. To the GTM-ICP, to Dr. Joaquín Pérez-Pariente, for receiving and advising E. Santiago during his stay. And to the UAM-A for the support in student mobility.

References

[1] J. Pariente, Biocombustibles, sus implicaciones energéticas, ambientales y sociales, Fondo de Cultura Económica, México, 2016.
[2] M. Ayoub, M.A. Zuhairi, Renew. Sust. Energ. Rev. 16 (2012) 2671–2686.
[3] A. Dima, K. Boura, A. Foukis, O.A. Gkini, E.M. Papamichael, Bioresour. Technol. 200 (2015) 178–185.
[4] R. Nanda, Y. Zhang, Z. Yuan, W. Qin, H. Ghaziaskar, C. Xu, Renew. Sust. Energ. Rev. 56 (2016) 1022–1031.
[5] R.A. Market, Glycerol market by source, by applications – global industry analysis, size, shar, trends, growth and forecast, Transparency Market Research Ireland, 2013 73.
[6] A. Galadima, O. Muraza, Waste Biomass Val 8 (2017) 141–152.
[7] OECD-FAO Agricultural Outlook 2015-2024, OECD publishing, Francia, 2015.
[8] Q. He, J. McNutt, J. Yang, Renew. Sust. Energ. Rev. 71 (2017) 63–76.
[9] Y. Gu, S. Liu, C. Li, Q. Cui, J. Catal. 301 (2012) 93–102.
[10] P.S. Kong, M.K. Aroua, W. Daud, Renew. Sustain. Energy Rev. 63 (2016) 533–555.
[11] F. Yang, M.A. Hanna, R. Sun, Biotechnol. Biofuels (2012) 5–13.
[12] C. Quispe, C. Coronado, J. Carvalho, Renew. Sustain. Energy Rev. 27 (2013) 475–493.
[13] C. Solarte, Obtención mediante procesos quimioenzimáticos de derivados del glicerol, Doctoral thesis for the Universitat de Lleida, Departamento de Química, Escola Técnica Superior d'Enginyeria Agrària, 2012.
[14] M. Anitha, S.K. Kamarudin, N.T. Kofli, Chem. Eng. J. 295 (2016) 119–130.
[15] S. Katryniok, V. Paul, P. Belliere-Baca, F. Dumeignil, Green Chem. 12 (2010) 2079–2098.
[16] S. Bagheri, N.M. Julkapli, W.A. Yehye, Renew. Sustain. Energy Rev. 41 (2015) 113–127.
[17] N. Rahmat, A.Z. Abdullah, A.R. Mohamed, Renew. Sustain. Energy Rev. 14 (2010) 987–1000.
[18] X. Luo, X. Ge, S. Cui, Y. Li, Bioresour. Technol. 215 (2016) 144–154.
[19] A.S. Olivera, S.J. Vasconcelos, J.R. Sousa, F.F. Sousa, J.M. Filho, A.C. Oliveira, Chem. Eng. J. 168 (2011) 765–774.
[20] A. Ulgen, W.F. Hoelderich, Appl. Catal. A-Gen. 400 (2010) 34–38.
[21] A. Talebian-Kiakalaieh, N.A. Amin, H. Hezaveh, Renew. Sustain. Energy Rev. 40 (2013) 28–59.
[22] B. Katryniok, S. Paul, M. Capron, C. Lancelot, V. Belliere-Baca, P. Rey, F. Dumeignil, Green Chem. 12 (11) (2010) 1922–1925.
[23] S.H. Chai, H.P. Wang, Y. Liang, B.Q. Xu, Green Chem. 9 (10) (2007) 1130–1136.
[24] S.H. Chai, H.P. Wang, Y. Liang, B.Q. Xu, Green Chem. 10 (10) (2008) 1087–1093.
[25] W. Suprun, M. Lutecki, R. Gläser, H. Papp, J. Mol. Catal. A Chem. 342–343 (1) (2011) 91–100.
[26] E. Yoda, A. Otawa, Appl. Catal. A Gen. 360 (1) (2009) 66–70.
[27] Y.T. Kim, K.D. Jung, E.D. Park, Microporous Mesoporous Mater. 131 (1–3) (2010) 28–36.
[28] L.H. Vieira, K.T.G. Carvalho, E.A. Urquieta-González, S.H. Pulcinelli, C.V. Santilli, L. Martins, J. Mol. Catal. A Chem. 422 (2016) 148–157.
[29] F. Cavani, S. Guidetti, L. Marinelli, M. Piccinini, E. Ghedini, M. Signoretto, Appl. Catal. B 100 (1–2) (2010) 197–204.
[30] S.H. Chai, H.P. Wang, Y. Liang, B.Q. Xu, J. Catal. 250 (2) (2007) 342–349.
[31] P. Lauriol-Garbey, J.M.M. Millet, S. Loridant, V. Belliere-Baca, P. Rey, J. Catal. 281 (2) (2011) 362–370.
[32] L.Z. Tao, S.H. Chai, Y. Zuo, W.T. Zheng, Y. Liang, B.Q. Xu, Catal. Today 158 (3–4) (2010) 310–316.
[33] A. Ulgen, W. Hoelderich, Catal. Lett. 131 (1) (2009) 122–128.
[34] P. Lauriol-Garbay, J.M.M. Millet, S. Loridant, V. Bellière-Baca, P. Rey, J. Catal. 280 (1) (2011) 68–76.
[35] Y. Liao, M. Fu, L. Chen, J. Wu, B. Huang, D. Ye, Catal. Today 216 (2013) 220–228.
[36] M. Martinez, Obtención de Acroleína a partir del glicerol utilizando como catalizador Pt/Alúmina mesoporosa, Master's Thesis, Universidad Autónoma Metropolitana, México, 2014.
[37] M. Garcia, Síntesis y caracterización de Pt soportado en óxido de cerio mesoporoso para la conversión de glicerol en productos de alto valor agregado. Master's Thesis, Universidad Autónoma Metropolitana, México, 2014.
[38] M. Massa, A. Andersson, E. Finocchio, G. Busca, J. Catal. 307 (2013) 170–184.
[39] Y.T. Kim, K.D. Jung, E.D. Park, Appl. Catal. B-Environ. 107 (1-2) (2011) 177–187.
[40] S. Larrondo, M.A. Vidal, B. Irigoyen, A.F. Craievich, D.G. Lamas, I.O. Fábregas, N. Amadeo, Catal. Today 107-108 (2005) 53–59.
[41] C. Márquez-Álvarez, N. Ziková, J. Perez-Parienté, J. Cejka, Catal. Rev. 50 (2008) 222–286.
[42] A. Trovarelli, Catalysis and Related Materials, Imperial College Press, London, 2002.
[43] S.J. Vasconcelos, C.L. Lima, J.M. Filho, A.C. Oliveira, E.B. Barros, F.F. de Sousa, M.G. Rocha, P. Bargiela, A.C. Oliveira, Chem. Eng. J. 168 (2011) 656–664.
[44] V. González, I. Díaz, C. Márquez-Álvarez, E. Sastre, J. Pérez-Pariente, Stud. Surf. Sci. Catal. 142 (2002) 1283–1290.

[45] N. Pernicone, F. Traina, B.E. Leach (Ed.), Commercial Catalysts Preparation, Applied Industrial Catalysis, Vol.3, Academic Press, New York, 1984p.1.
[46] M. Trueba, S.P. Trasatti, Eur. J. Inorg. Chem. (2005) 3393–3403.
[47] J.T. Miller, M. Schreier, A.J. Kropf, J.R. Regalbuto, J. Catal. 225 (2004) 203–212.
[48] M.L. Hernández, L.C. Caero, Caracterización de Catalizadores, México, (2014).
[49] J. Roggenbuck, H. Schafer, T. Tsoncheva, C. Minchev, J. Hanss, M. Tiemann, Microporous Mesoporous Mater. 101 (2007) 335–341.
[50] K. Tanabe, M. Misono, Y. Ono, H. Hattori, Stud. Surf. Sci. Catal. 51 (1989) 5–25.
[51] H.S.A. de Sousa, de Assis Barros, S.J.S. Vasconcelos, J.M. Filho, C.L. Lima, A.C. Oliveira, A. Ayala, M. Junior, A. Oliveira, Appl. Catal. A Gen. 406 (2011) 63–72.
[52] C.L. Lima, H.S.A. de Sousa, S.J.S. Vasconcelos, J.M. Filho, A.C. Oliveira, F.F. de Sousa, A.C. Oliveira, Reac. Kinet. Mech. Catal 102 (2) (2011) 487–500.
[53] M. Brigante, P.C. Schulz, J. Colloid Interf Sci 369 (2012) 71–81.
[54] G. Urretavizcaya, A.L. Cavalieri, J.M. Porto Lopez, I. Sobrados, J. Sanz, J. Mat. Synthesis Process 6 (1998) 1–7.
[55] Shuichi Arakawa, Yoko Matsuura, Masami Okamoto, Appl. Clay Sci. 95 (2014) 191–196.
[56] G.S. Foo, D. Wei, D.S. Sholl, C. Sievers, ACS Catal. 4 (9) (2014) 3180–3192.
[57] A. Kinage, P. Upare, P. Kasinathan, Y.K. Hwang, Jong-San Chang, Catalan J. Commun. Cult. Stud. 11 (2010) 620–623.
[58] V. Montes, M. Checa, A. Marinas, M. Boutonnet, J.M. Marinas, F.J. Urbano, S. Järas, C. Pinel, Catal. Today 223 (2014) 129–137.
[59] E. Bozga, V. Plesu, G. Bozga, C.S. Bildea, E. Zaharia, Rev. chim. (Bucharest) 62 (6) (2011) 646–654.
[60] J. Baneshia, M. Haghighia, N. Jodeiria, M. Abdolahifara, H. Ajamein, Ceram. Int. 40 (2014) 14177–14184.
[61] M. García, J. Aguilar, L.E. Noreña, C. Márquez, J. Pérez, N.C. Martin Guaregua, J. Appl, Res. Technol. 16 (2018) 511–523.
[62] L.F. Liotta, A. Longo, A. Macaluso, A. Martorana, G. Pantaleo, A.M. Venezia, G. Deganello, Appl. Catal. B: Env. 48 (2004) 133–149.
[63] M. Martínez-Rico, J. Aguilar Pliego, J. Pérez-Pariente, C. Marquez, M. Viniegra, N. Martin, RMIQ 17 (2) (2018) 523–532.
[64] S. Sato, M. Akiyama, R. Takahashi, T. Hara, K. Inui, M. Yokota, Appl. Catal. A Gen. 347 (2008) 186–191.